Applied Catalysis B: Environmental 88 (2009) 42–49

Contents lists available at ScienceDirect

Applied Catalysis B: Environmental

journal homepage: www.elsevier.com/locate/apcatb

MgCoAl–LDH derived heterogeneous catalysts for the ethanol transesterification of canola oil to biodiesel

Eugena Li [a], Zhi Ping Xu [b], Victor Rudolph [a,*]

[a] Chemical Engineering Department, University of Queensland, St. Lucia, QLD 4072, Australia
[b] ARC Centre for Functional Nanomaterials, Australian Institute of Bioengineering and Nanotechnology, University of Queensland, St Lucia, QLD 4072 Australia

ARTICLE INFO

Article history:
Received 7 May 2008
Received in revised form 1 September 2008
Accepted 21 September 2008
Available online 2 October 2008

Keywords:
Biodiesel
Heterogeneous catalyst
Layered double hydroxide
Cobalt
Transesterification of canola oil
Ethanol

ABSTRACT

Mixed oxide catalysts derived from Mg–Co–Al–La layered double hydroxide (LDH) with various Mg:Co:Al:La ratios were prepared by co-precipitation and calcination. Their catalytic performance as heterogeneous base catalysts for the transesterification of canola oil with ethanol to produce biodiesel was compared over 5 h in a batch reactor at 473 K. Amending the catalyst by the addition of La, a possible stabilizer and catalyst, and an increase in Mg, which provides the main base catalyst sites, did not seem to affect the catalytic activity. Experiments using Mg_2CoAl catalyst are reported, showing the effects of reaction temperature, ethanol-to-oil molar ratio, particle size, and catalyst stability in the transesterification of canola oil. The catalytic activity of the Mg_2CoAl was demonstrated and shown to be stable and reusable maintaining its activity after 7 cycles. The kinetics of the transesterification of canola oil catalyzed by Mg_2CoAl may be modeled as a first-order reaction.

1. Introduction

Biodiesel, derived from biological resources such as vegetable oils and animal fats, is accepted in many countries as an extender or substitute for fossil based diesel, having the advantages of being biodegradable and nontoxic, with an environmentally friendly emission profile. Biodiesel possesses physiochemical properties very similar to those of petroleum-based diesel, and thus provides a convenient alternative energy source for diesel engines using current supply chains [1].

Biodiesel is commonly produced via transesterification of vegetable oils or animal fats with an alcohol, most often using a catalyst intermediary. Transesterification has been carried out most frequently over basic catalysts such as sodium or potassium hydroxide, methoxide, or carbonate in industries, mainly due to its fast reaction rate [2]. However, this homogeneous base-catalyzed system is sensitive to water and free fatty acids (FFA) that are often present in lower grade and cheaper feedstock oil, resulting in the formation of emulsions and the generation of waste water during product separation [3]. Therefore, increased research efforts have been directed towards the development of heterogeneous catalyst systems to produce biodiesel in recent years as reviewed in [4]. Their benefits include simplification of the separation and purification of the reaction products, easy reuse of the catalyst in the reactor, and possibly low sensitivity to FFAs and water.

Layered double hydroxides (LDHs) are known as anionic clays and widely used as adsorbents, ion exchangers, base catalysts, and precursors of mixed oxides for various catalytic applications. Most LDHs adhere to the general chemical formula: $[M^{II}_{1-x}M^{III}_x(OH)_2]^{x+}(A^{n-})_{x/n}\cdot mH_2O$, where M^{II} represents any divalent metal cation, M^{III} any trivalent metal cation and A^{n-} an anion (inorganic or organic) [5,6]. As LDHs can contain more than two types of metal cations at various ratios, one can rationally design and synthesize particular LDHs and the derived mixed oxides with desirable catalytic properties for the target reaction. For example, LDHs and the derived mixed oxides have been used as heterogeneous catalysts for oil transesterification. Cantrell et al. [7] investigated the activity of a series of $[Mg_{(1-x)}Al_x(OH)_2]^{x+}(CO_3)_{x/n}^{2-}$ LDH materials with compositions over the range of $0.35 < x < 0.55$ for biodiesel production. They were all found to be effective catalysts for the transesterification of glyceryl tributyrate with methanol, with a conversion ranging from 42.4% to 74.8% after 3 h reaction at 333 K. In a study conducted by Xie et al. [8], Mg–Al LDH with an Mg/Al ratio of 3.0 derived from calcination at 773 K was found to be the optimum catalyst resulting in a conversion of 67% when the reaction was carried out at a 15:1 methanol-to-soybean oil molar ratio with a

* Corresponding author. Tel.: +61 7 33654171; fax: +61 7 33654199.
E-mail address: v.rudolph@uq.edu.au (V. Rudolph).

0926-3373/$ – see front matter © 2008 Elsevier B.V. All rights reserved.
doi:10.1016/j.apcatb.2008.09.022

catalyst loading of 7.5 wt% at the reflux temperature for 9 h. Calcined $[LiAl_2(OH)_6](CO_3)_{0.5}\cdot nH_2O$ was also reported to be an effective catalyst for the transesterification of soybean oil with methanol in a study conducted by Shumaker et al. [9] in which a methyl ester yield of over 80% was produced when the catalyst was calcined at 723 K, and the reaction was conducted at a methanol-to-oil ratio of 15:1 with a catalyst loading of 1 wt% at the reflux temperature for 1 h.

In this study, canola oil (a.k.a. rapeseed oil) was used as the feedstock. Canola is a popular biodiesel feed material because it produces more oil per unit of land area as compared to other oil sources [10] and the seeds have a high oil content of about 40%, simplifying oil recovery. Many studies have investigated the transesterification reaction of canola oil for biodiesel production. Most pertinently, Gryglewicz showed that the transesterification of canola oil can be catalyzed effectively by basic alkaline-earth metal compounds [11]. MacLeod et al. evaluated a series of alkali-doped metal oxides for their activity in the transesterification of rapeseed oil to biodiesel and found a conversion of over 90% in a standard 3 h test [12]. These studies used methanol as the alcohol reactant because of its relatively low cost and easy availability. In addition, methanol does not form an azeotrope with water and therefore excess reactant is easily recovered for reuse.

In this study, however, we chose to use ethanol instead of manufactured methanol because ethanol is less toxic, less volatile and less corrosive, providing a safer work environment during the transesterification process. Moreover, ethanol is readily available from fermentative processes using biomass feedstocks (e.g. corn and sugar cane), making ethanol biodiesel production, in principle, fully independent of fossil-derived energy and renewable [13,14].

In our preliminary catalytic tests, calcined Mg_3Al–LDH was found to be very active as a heterogeneous catalyst in the transesterification of canola oil and ethanol for biodiesel synthesis. This catalyst, however, turned into a gel-like substance during the reaction, making recovery and reuse very difficult. To improve this situation, we designed and synthesized several new mixed oxide catalysts derived from their LDH precursors. Cobalt and lanthanum were incorporated into the derived mixed oxides to promote the formation of spinel phase with the expectation that this would stabilize the morphology and structure during the application [15–17]. In addition, cobalt and lanthanum may themselves catalyze or promote the desired reactions [18–20].

Our experiments showed that these mixed oxide catalysts are very active in the transesterification of canola oil with ethanol. Catalyst Mg_2CoAl was found to be readily recovered for reuse and showed no reduction in activity over 7 reaction cycles. This catalyst was then further investigated, as elaborated below.

2. Experimental

2.1. Materials

Commercial edible grade canola oil was purchased from the supermarket. Analytical reagent grade 99.5% ethanol (Ajax) was used for the transesterification reactions. NaOH (≥97%), Na_2CO_3 (≥99.8%), $Mg(NO_3)_2\cdot 6H_2O$ (≥99%), $Al(NO_3)_3\cdot 9H_2O$ (≥98%), $Co(NO_3)_2\cdot 6H_2O$ (≥98%) and $La(NO_3)_3\cdot 6H_2O$ (≥99.99%) used to synthesize the catalysts were purchased from Sigma–Aldrich Pty Ltd., Australia.

2.2. Catalyst preparation

The mixed oxide catalysts denoted as $Mg_xCoAl_yLa_z$ ($x = 2$ or 3 and $y + z = 1$) were prepared by calcining their precursors $Mg_xCoAl_yLa_z$–LDHs. These LDH materials were synthesized by a co-precipitation method. Briefly, 50 mL of mixed salt solution containing $0.2x$ M $Mg(NO_3)_2\cdot 6H_2O$, 0.2 M $Co(NO_3)_2$, $0.2y$ M $Al(NO_3)_3\cdot 9H_2O$ and $0.2z$ M $La(NO_3)_3$ was added into 200 mL a mixed base solution containing 0.4 M NaOH and 0.026 M Na_2CO_3. A precipitate formed and the mixture was aged to 353 K under continuous stirring for 6 h. The mixed suspension was then cooled down, and the LDH precipitate was separated and washed with deionized water via centrifugation. The collected LDH was dried at 373 K overnight and calcined at 873 K for 4 h at a heating rate of 10 K/min. All calcined catalysts were ground to a powder form prior to use, with a mean particle size of less than 100 μm.

The Mg_3Al–LDH used in the preliminary test was prepared in a similar way as described above, except that no Co or La was added, and the formed LDH calcination was done at 773 K. The resulting catalyst was in a powder form where no additional grinding was required.

2.3. Catalyst characterization

The X-ray diffraction (XRD) patterns of the precursors and catalysts were recorded on a Bruker D8 Advance X-Ray Diffractometer equipped with a graphite monochromator, copper radiation, and scintillation counter (detector) in the range of $2\theta = 5$–80° with a resolution of 0.02° at a scanning rate of 0.5°/min. Traces were analyzed using the Diffrac^{plus} Evaluation Package Release 2006 Version 12.0 and PDF (Powder Diffraction File)-2 Release 2006. The atomic concentrations on the catalyst surface (up to 10 nm) were acquired using a Kratos Axis ULTRA X-ray Photoelectron Spectrometer incorporating a 165 mm hemispherical electron energy analyzer. The incident radiation was monochromatic Al X-rays (1486.6 eV) at 225 W (15 kV, 15 mA). Survey scans were taken at an analyzer pass energy of 160 eV and carried out over a binding energy ranging from 1200 to 0 eV with a step size of 1.0 eV and a dwelling time of 100 ms. The surface area and porosity of the derived catalysts were measured by N_2 adsorption/desorption using a Quadrasorb SI Surface Area and Pore Size Analyzer (Quantachrome Instruments). Before each N_2 adsorption/desorption measurement, the catalyst was heated under vacuum at 473 K overnight in a Quantachrome FloVac Degasser to desorb any impurities that might have adsorbed onto the solid during exposure to air. The particle size distributions of the ground catalyst powders were measured by the Mastersizer 2000 (Malvern Instruments) particle size analyzer with a Hydro MU large volume manual sample dispersion unit, whereas that of the unground Mg_2CoAl particles as synthesized was obtained by Endecotts test sieves.

Chemisorption of acidic carbon dioxide was performed using an Autosorb-1-C Chemisorption-Physisorption Analyzer (Quantachrome Instruments). Each catalyst was degassed under vacuum at 473 K overnight in a Quantachrome FloVac Degasser, and then transferred to the sample cell of the analyzer and was heated to 473 K at a rate of 5 K/min under vacuum. CO_2 adsorption was performed at 2 pressure points (5 and 760 mm Hg) at 473 K.

2.4. Reaction procedures

2.4.1. Catalytic tests

Fifty grams of canola oil, 43 g of ethanol (equivalent to ca. 16:1 ethanol-to-oil molar ratio), and 1.0 g of catalyst (2 wt%) were loaded into a Parr 4560 Mini Bench Top Reactor at room temperature. The mixture was heated under vigorous stirring at an average rate of ca. 7 K/min to 473 K, at which the pressure reached 25 atm. The reaction temperature was then maintained at 473 K for 300 min. Sampling began once the reaction temperature reached 473 K (recorded as the starting time, t_0), where a sample of

about 2 mL was extracted from the reactor using a stainless steel sampling bomb assembled with Swageloks and pressure valves. A series of samples were then extracted at various time intervals until t = 300 min. Once a sample (2 mL) was taken, the sampling bomb was immediately placed into an ice bath to cool down for about 10–15 min. The sample was then pushed by syringe through a 0.22 μm millipore filter unit into a glass vial, to remove any catalyst particles prior to GC analysis.

The Mg_2CoAl was selected on the basis of performance to investigate the influences of particle size, ethanol-to-oil molar ratio and reaction temperature on the ethyl ester yield. The experiments were conducted at ethanol:oil ratios of 7:1, 8:1, 11:1, 14:1, and 16:1, respectively, and the reaction temperature was varied between 413 and 473 K.

2.4.2. Analytical methods

100 ± 0.1 mg of each liquid sample from the filtered reaction mixture was weighed into a 10 mL septa vial, derivatized with N-Methyl-N-(trimethylsilyl)trifluoroacetamide (derivatization grade, Aldrich) for approximately 15 min, and then diluted in heptane for GC analysis as described in ASTM Method D6584 [21]. The ester and glyceride concentrations in the liquid samples were determined by a Varian CP 3900 Gas Chromatograph equipped with an FID detector, an on-column injector and a CP 7491 column (15 m long, 0.320 mm ID). The canola oil conversions were estimated based on the isolated yield of C18 esters, namely ethyl linolenate, linoleate, oleate and stearate, representing the major components in canola oil. These are convenient characteristic markers, since they were each individually calibrated against certified standards in the GC.

2.4.3. Catalyst stability tests

When the 5-h transesterification reaction was completed, the reactor was cooled to room temperature and the catalyst, Mg_2CoAl, was collected from the reaction mixture through filtration. It was then dried in an oven at 383 K overnight and stored in a desiccator without any further treatment until it was reused for the stability test. The same amounts of fresh canola oil (50 g) and ethanol (43 g) were added to the recycled catalyst each time to react under the same conditions. The repeated tests were conducted for 7 reaction cycles.

3. Results and discussion

3.1. Physiochemical characterization of catalysts

Four mixed oxide catalysts were prepared, as listed in Table 1. The surface atomic ratio of Mg:Co:Al:La determined by XPS is very close to the designed ratio in the LDH precursor phase, indicating that calcination does not cause any significant segregation of the metal elements onto the surface. Mg_3Al oxide derived from its LDH form was also prepared as a catalyst (not shown in Table 1), but was not extensively tested because it was found to be unrecoverable and was thus not suitable for heterogeneous catalysis. Nevertheless, where informative, some of its characteristics are mentioned in the following section.

Table 1
Physical characteristics of calcined LDH catalysts[a].

Catalyst	N_2 adsorption/desiorption			[b]CO_2 adsorption (mmol/g)	
	S (m^2/g)	w (nm)	V (cm^3/g)	At 5 mm Hg	At 760 mm Hg
Mg_2CoAl	89.0	6.7	0.291	0.13	0.31
$Mg_3CoAl_{0.9}La_{0.1}$	60.9	11.9	0.371	0.15	0.38
$Mg_2CoAl_{0.9}La_{0.1}$	75.7	10.3	0.400	0.10	0.26
$Mg_2CoAl_{0.7}La_{0.3}$	58.1	10.1	0.293	0.08	0.26

[a] Pore diameter w was calculated using the nitrogen adsorption data by BJH method; S is the BET surface area; and V is the pore volume.
[b] Standard gas at 298 K.

The Brunauer–Emmett–Teller (BET) surface area, pore size calculated from the adsorption branch by the Barrett–Joyner–Halenda (BJH) model, and pore volume of the as-prepared catalysts are presented in Table 1. All four catalysts have a medium specific surface area (58–89 m^2/g) and pore volume (0.29–0.40 cm^3/g) with mesoporous structure (6.7–11.9 nm). It is noted that Mg_2CoAl showed a slightly larger surface area, but smaller pore size and pore volume than the other catalysts. This suggests that the addition of La has a tendency to reduce surface area while increasing pore size and pore volume of the catalysts. The nitrogen adsorption/desorption isotherms obtained for all catalysts were type IV with an H1 hysteresis loop, indicative of large channel-like interparticle pores with a narrow size distribution.

The amount of CO_2 uptake per gram of catalyst at the low pressure indicates the relative basic strength; the uptake at the high pressure characterizes the total number of basic sites. The basic strength and the total number of basic sites on the surface are similar among all the catalysts, but appear to be dependent on the content of Mg in the catalysts. This is supported by the fact that $Mg_3CoAl_{0.9}La_{0.1}$, which contains the largest amount of Mg, adsorbs 20–50% more CO_2 than other catalysts at both pressures. Moreover, the introduction of La seems to cause a slight reduction in the amount of CO_2 adsorption as Mg_2CoAl adsorbed more CO_2 at both pressures than $Mg_2CoAl_{0.9}La_{0.1}$ and $Mg_2CoAl_{0.7}La_{0.3}$.

Fig. 1 illustrates the XRD patterns of the mixed oxide catalysts and one LDH precursor. The LDH precursor, representative of all four LDHs, shows typical diffraction peaks of the LDH layered structure, as indexed with (0 0 3), (0 0 6) and (1 1 0) [22]. It is observed that the diffraction patterns of the derived oxide catalysts are totally different from those of the precursor, demonstrating a complete transformation from LDH phase to the oxide phase after calcination at 873 K for 4 h. The mixed oxides are mainly of spinel type and salt rock (MgO) type. For example, Mg_2CoAl shows diffraction peaks at $2\theta \approx 19^\circ$, 31°, 37°, 45°, 60°, and 66° which are characteristic of spinel phase [23] and at $2\theta \approx 43^\circ$ and 63° which identify the rock phase (MgO) [24]. Characteristic peaks of lanthanum oxide (La_2O_3) are observed in the La-containing oxide catalysts, particularly evident in sample $Mg_2CoAl_{0.7}La_{0.3}$, as marked in Fig. 1.

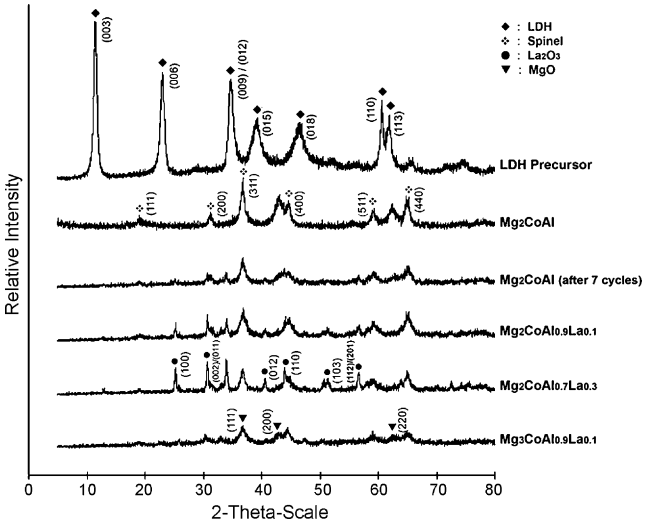

Fig. 1. Large angle XRD patterns of LDH catalysts.

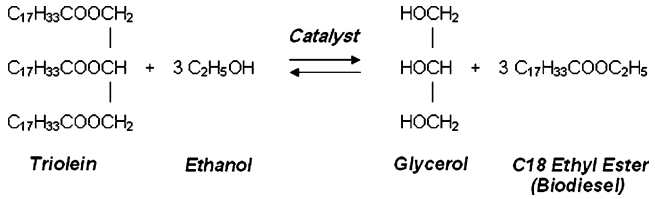

Scheme 1. The transesterification of triolein (glycerol trioleate) to C18 ethyl esters.

3.2. Catalyst performance

The initial composition of the canola oil used as a starting material was analyzed by the GC. It contained 87 wt% of combined C18 fatty acids, with approximately 12 wt% palmitic acid (C16:0), and 1 wt% eicosenoic acid (C22:1). Therefore, the performance of the mixed oxide catalysts were compared on the basis of oil conversion estimated from their combined C18 ethyl ester yield, which represents almost 90% of the ester contents. Using triolein (a triglyceride made up of C18 fatty acids) and ethanol as an example, transesterification involves 3 reversible reactions that progressively converts triolein to diolein to monoolein to glycerol, yielding one C18 ethyl ester molecule at each step. The overall reaction is represented in Scheme 1. The three reactions are commonly catalyzed by a base catalyst, provided here as a solid mixed oxide.

Fig. 2A shows the concentration profile of C18 ethyl esters in the catalyst tests using the 4 oxide catalysts, in comparison with that of the control experiment conducted without any catalyst. Since the time recording started only when the reaction temperature was reached ($t = 0$), it should be noted that for all the catalysts, a significant amount of ethyl esters (4–10%) had already been produced during the heating period from room temperature to 473 K (ca. 30 min). For the control experiment, C18 ethyl esters were not observed until $t = 60$ min, and only a small amount (<5%) was generated by the time $t = 180$ min. By contrast, over 90% C18 ethyl esters were produced within 180 min when using the catalysts.

The evolving distribution profiles of the glycerides (namely monoolein, diolein, and triolein) with reaction time are shown in Fig. 2B–D. Our GC results reveal that the unreacted canola oil itself contains ca. 8% diolein, which explains the ca. 92% triolein concentration at $t = 0$ in the case of the control experiment (no catalyst) in Fig. 2D. Without catalyst, the triolein consumption was only ca. 22% over the whole 5 h recording period. On the other hand, when catalyst was used, there was almost complete conversion of triolein after $t = 120$ min, and no triolein left after $t = 180$ min. The diolein concentration remained quite constant at ca. 8% throughout the recording period in the case of the control experiment, but it steadily decreased from 6–8% to <1% within 150 min when a catalyst was used (Fig. 2C). It may be the case that the diolein concentration had already peaked during the heating period when the catalysts were used.

The monoolein concentration profiles were quite similar in all 4 catalyst cases, peaking at ca. 90 min (6–8%) and slowly decreasing to 1–4% in 210 min. As intermediate species, the monoolein and diolein together made up only a small portion of the reaction mixture, suggesting that they were being converted to the final products (C18 ethyl esters and glycerol) at a relatively rapid rate.

In terms of yield, all 4 catalysts have very similar catalytic activity. La was expected to enhance the catalytic activity, but the effect could not be unambiguously discerned in this study. Moreover, no direct correlation was found between the basicity of the catalysts (Table 1) and their catalytic activity to yield C18 ethyl esters, which is contrary to the findings in our previous study on MgO-functionalized SBA-15 catalysts [25]. The marginal difference in the catalytic activity demonstrated by these catalysts show hardly any effects of La or an enhanced Mg concentration under the experimental conditions that were used.

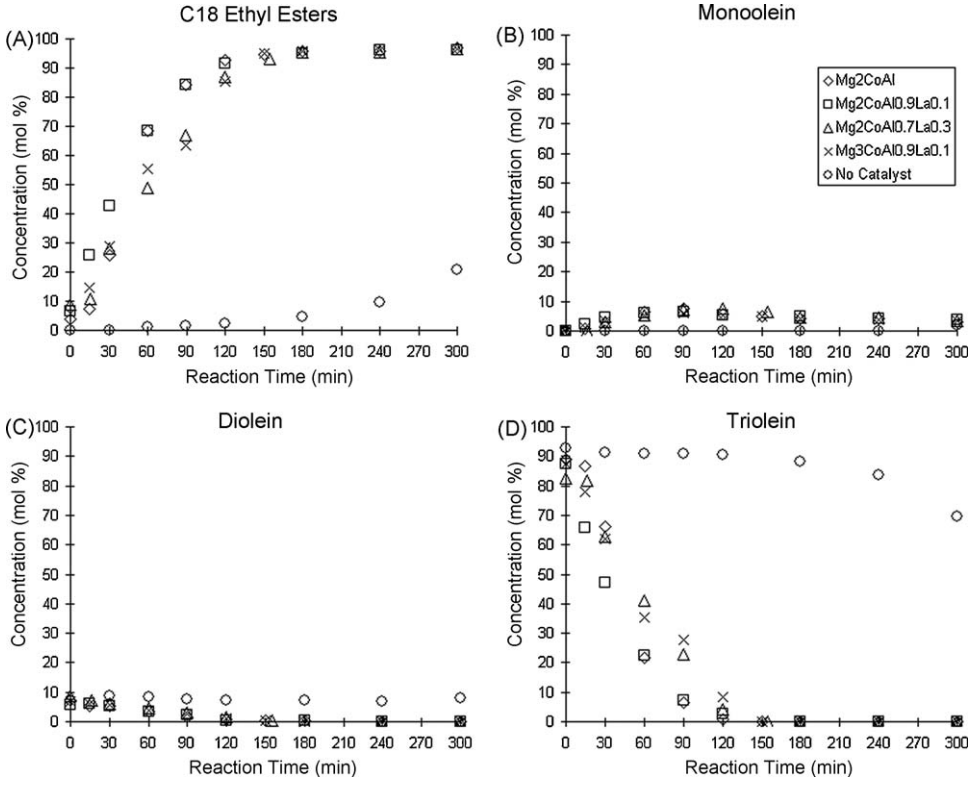

Fig. 2. Concentration profiles of the transesterification of canola oil catalyzed by different catalysts.

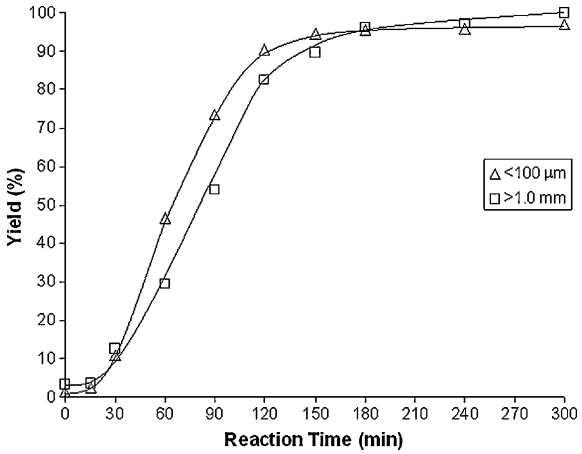

Fig. 3. Effect of particle size on catalytic activity.

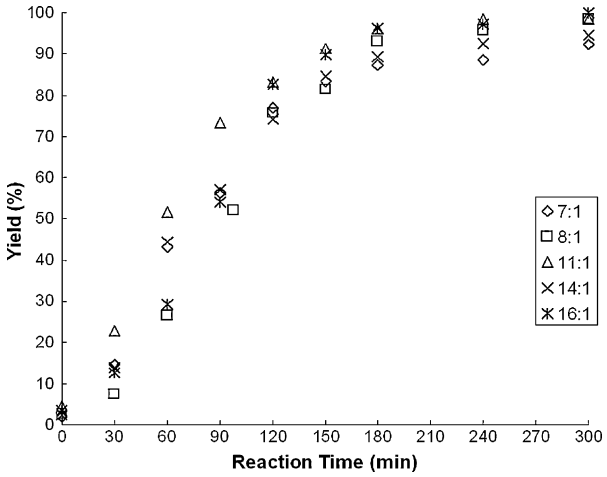

Fig. 4. Effect of alcohol-to-oil molar ratio on catalytic activity.

In the following sections, Mg_2CoAl has been chosen as an example to investigate further the effects of various reaction parameters on the catalytic performance.

3.3. Catalyst particle size

In order to investigate possible rate constraints due to internal diffusion in the LDH-derived oxide catalysts, a comparison was made of conversion rates for different catalyst particle sizes. Mg_2CoAl particles with diameter larger than 1.0 mm were used as synthesized (without grinding) to catalyze the reaction under the same conditions as the ground material. A reduction in conversion rate with particle size indicates internal diffusion control.

Fig. 3 shows that the rate (given by the slope of the curves) is very similar for both sizes, e.g. during the period from about 30–90 min, but with a notable lag of about 15 min for the larger particles. The consistency in the rates indicates that the conversion rate is controlled by chemical kinetic considerations rather than internal diffusion. The reason for the lag is more difficult to explain. We speculate that this lag may be due to the phase separation effects within the system. Canola oil and ethanol are not fully miscible, but the miscibility increases as biodiesel is formed in the system. Reduced access by larger colloidal oil droplets to internal catalyst sites in the larger Mg_2CoAl particles may hinder reaction early on, until a sufficient biodiesel concentration is built up (even locally) to promote miscibility. Thereafter, the reaction is controlled by the chemical kinetics. However, further studies will be required to verify this speculative explanation.

3.4. Effect of ethanol-to-oil ratio

According to the reaction shown in Scheme 1, one mol of triolein reacts with 3 mol of ethanol to produce 3 mol of C18 ethyl esters and 1 mol of glycerol. In practice, excess alcohol is typically applied to increase oil conversion by shifting the reaction equilibrium, and as such, the C18 ethyl ester yield is expected to increase with an increase in the amount of ethanol used. Such a trend is generally observed in Fig. 4, where the highest ethanol:oil ratio of 16:1 led to the highest yield, and the smallest ratio of 7:1 the lowest yield after 5 h. However, the reaction rate estimated by the slope of the curves for all ethanol-to-oil ratios was found to be quite similar, possibly because the effect of the ethanol:oil ratio was compromised by the influences of the extreme reaction conditions (i.e. 473 K and vigorous stirring), and therefore became less obvious.

3.5. Reaction temperature

Fig. 5 shows the C18 ethyl ester yields at 5 reaction temperatures, 413, 433, 443, 453 and 473 K using an ethanol-to-oil molar ratio of 16:1 and Mg_2CoAl as the catalyst. As the reaction temperature decreased, the conversion rate of the intermediate species also showed a corresponding decrease; thus a higher accumulation of diolein content was observed at lower reaction temperatures. For instance, at t = 180 min, all diolein had been converted at 473 K, but 3%, 13%, 16% and 29% diolein still remained at 453, 443, 433 and 413 K, respectively (Fig. 5C). In addition, the monoolein level was very low, not exceeding 8% in all cases throughout the whole recording period (Fig. 5B). This suggests that the conversion of diolein to monoolein is more sensitive to temperature than the conversion of monoolein to glycerol and that of triolein to diolein.

3.6. Reaction kinetics

The reaction time and temperature dependencies allow the kinetics of transesterifying canola oil to ethyl esters to be determined. The transesterification reaction involves 3 steps. However, for simplicity, a reasonable mathematical model may be based only on the overall reaction, as demonstrated in Scheme 1, and ignoring the intermediate reactions. If the overall reaction is taken to follow first-order kinetics, the rate constant as proposed by Kusdiana and Saka [26] can be determined based on the decreased amount of unethyl esterified compounds (uEC), which include trioleins, dioleins, and monooleins in this case, as given by Equation (1)

$$\text{Rate} = k[\text{uEC}] = -\frac{\text{d}[\text{uEC}]}{\text{dt}} \quad (1)$$

where [uEC] refers to the content of all glyceride species that result or remain at time t, and k is the overall rate constant. Integration of Equation (1) gives

$$-\ln \frac{\text{uEC},t}{\text{uEC},0} = kt \quad (2)$$

or

$$\ln [\text{uEC}, t] = -kt + \ln [\text{uEC}, 0] \quad (3)$$

Fig. 6A shows the correlation between the content of unethyl esterified compounds and the reaction time at various tempera-

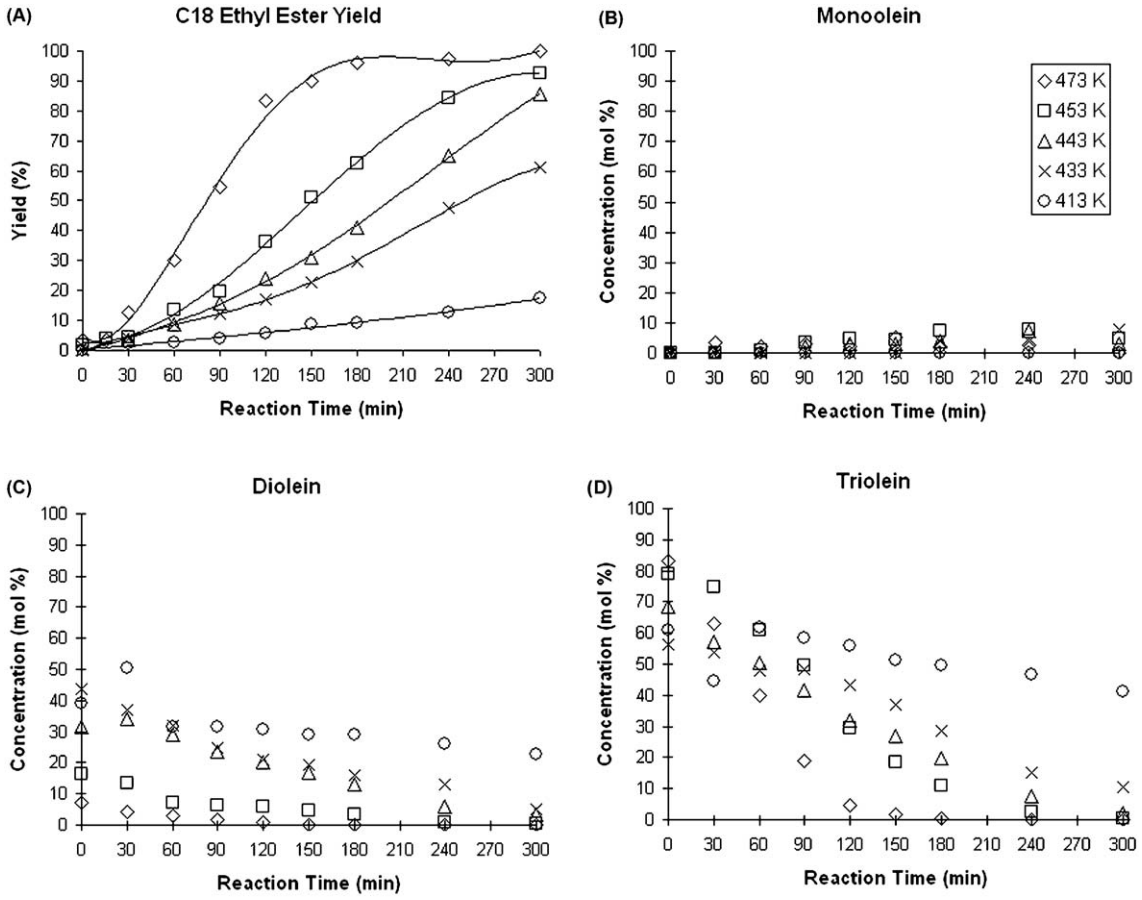

Fig. 5. Effect of reaction temperature on (A) yield and (B–D) glycerides distribution.

tures between 413 and 473 K. The plots of ln[uEC] vs. reaction time (t) are acceptably represented by straight lines, validating the first-order reaction model. However, it should be noted that this first-order model applies only to the initial stage of the reaction and the plot of ln[uEC] against time is linear only up to a conversion of ca. 90%. Only the relevant data points were included in Fig. 6A. The slopes of the lines provide the rate constants (k) with the units of s^{-1} and are used to determine the activation energy (E_a) by using the Arrhenius equation:

$$\ln(k) = \frac{-E_a}{RT} + \ln(A) \tag{4}$$

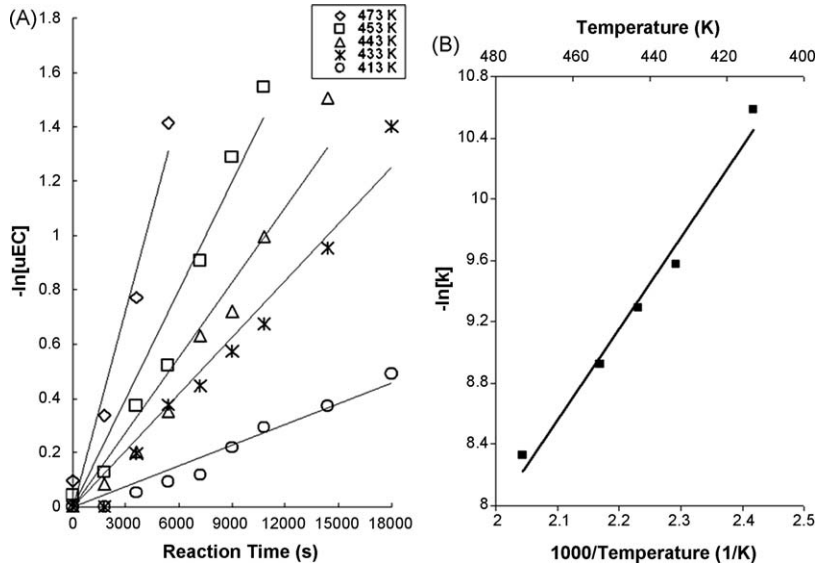

Fig. 6. (A) First-order reaction model of triolein transesterification (Eq. (3)) at various temperatures. (B) Arrhenius plot of reaction rate vs. temperature for transesterification reactions (Eq. (4)).

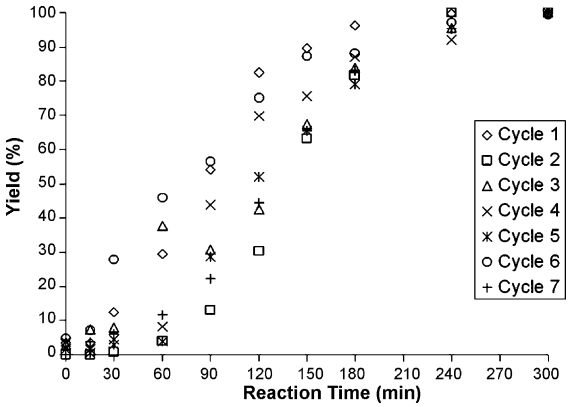

Fig. 7. Stability of Mg_2CoAl catalyst.

where R is the gas constant and A is the pre-exponential factor. The activation energy as calculated from the slope of the plot in Fig. 6B was found to be 60.5 kJ/mol, which is consistent with the range of 8–18.5 kcal/mol (equivalent to 33.5–77.5 kJ/mol) for the transesterification of soybean oil catalyzed by NaOH reported by Noureddini and Zhu [27].

3.7. Catalyst stability

Catalyst stability was tested by the simple method of recovering solids by filtration from the reactor after an experiment, drying overnight at 100 °C and holding in a dessicator until the next experiment. The results of 7 cycles are shown in Fig. 7. There is a great deal of scatter in the results, particularly in the first 180 min. We attribute the scatter to the uncontrolled methods used in catalyst recovery and handling between the tests. For instance, the mass of the dried catalyst retrieved from cycle 1 was 1.09 g, a nearly 10% mass increase from occluded or sorbed material from the previous reaction. Nevertheless, in an overall sense, the yield was quite similar, reaching a similar plateau at 95 ± 5% in all cycles. The tests demonstrate that catalyst Mg_2CoAl does not lose its activity in 7 cycles, indicating its relatively high stability. This is in contrary to the catalyst Mg_3Al, which exhibited a similar catalytic performance in the transesterification, but became a gel-like material after the reaction that was difficult to be recovered for reuse. The stability in the catalytic activity and morphology of catalyst Mg_2CoAl could be attributed to its major phase component, the spinel. As indicated in Fig. 1, the XRD pattern of Mg_2CoAl collected after 7 cycles is very similar to that of the initial unused Mg_2CoAl, except for the loss of most of its minor phase (rock salt, MgO).

A continuous packed bed reactor for which the catalyst is being developed would provide a better long term test of the catalyst and is in preparation.

4. Conclusions

LDH provides a suitable substrate for the preparation of metal oxide biodiesel catalysts. Although Mg_3Al was found to be active in catalyzing the transesterification reaction in our preliminary tests, it disintegrated into a gel-like material after the 5 h reaction and was unrecoverable for reuse. Therefore, the stability of the solid catalyst is very important, especially when it is applied in a fixed bed mode in which the catalyst is operated for long periods of time. The results from this study confirm that the stability of LDH catalysts can be achieved by suitable incorporation of Co and La to promote the formation of the spinel phase. All four Mg–Co–Al–La mixed oxide catalysts maintained their morphology, while exhibiting high yields of 96–97% when the transesterification was conducted at 473 K with an ethanol-to-oil ratio of 16:1 and a catalyst loading of 2 wt%. In the stability test with Mg_2CoAl, no major loss in activity was detected in the transesterification even after 7 cycles. No correlation has been found between the activity and the basicity or surface Mg concentration of the mixed oxide catalysts under the described conditions. Our results also show that the addition of La or an increased Mg concentration has limited influence on their catalytic performance.

Variations of several experimental parameters in the experiments with Mg_2CoAl show that the reaction temperature has a dominant effect on the catalytic performance. As expected, the ester yield and reaction rate increase with the reaction temperature. The glyceride distributions during transesterification are also greatly affected by temperature as our results indicate high accumulations of diolein in the system at lower temperatures. This implies that the conversion of diolein to monoolein slows down more than the other reaction steps as the temperature decreases.

The final yields for the different ethanol:oil ratios are in good agreement with the expected outcome, demonstrating higher yields at higher ethanol:oil ratios after 5 h, except in the case of 14:1. However, the high reaction temperature at 473 K might have compromised for some of the effects of the ethanol:oil ratio so that the expected difference in reaction rate was not observed in Fig. 4.

A reduction in conversion rate with particle size indicates internal diffusion control, but only when the phase separation effects are speculated to be significant within the system initially. As the miscibility of canola oil and ethanol increases with the formed biodiesel, the internal diffusion resistance diminishes, and thereafter, the reaction is controlled by the chemical kinetics. Further studies will, however, be required to verify this speculated explanation. Based on our simplified mathematical model, the overall reaction rate for the transesterification of canola oil catalyzed by Mg_2CoAl follows the first-order kinetics and the activation energy is estimated to be 60.5 kJ/mol.

Acknowledgements

This work has been funded by the ARC Linkage Grants Program with contributions by industrial sponsor IOR Energy Pty Ltd. The authors thank Mrs. Anya Yago for her assistance in XRD analyses.

References

[1] Tyson, K.S.a.M., R.L., Biodiesel Handling and Use Guidelines, third ed., National Renewable Energy Laboratory (2006).
[2] F. Ma, M.A. Hanna, Bioresour. Technol. 1 (1999) 1–15.
[3] J.M. Marchetti, V.U. Miguel, A.F. Errazu, Renewable Sustainable Energy Rev. 6 (2007) 1300–1311.
[4] U. Schuchardt, R. Sercheli, G. Gelbard, J. Braz. Chem. Soc. (1998) 199–210.
[5] P.S. Braterman, Z.P. Xu, F. Yarberry, Handbook of Layered Materials, Marcel Dekker, Inc., New York, 2004, pp. 373–474.
[6] F. Cavani, F. Trifiro, A. Vaccari, Catal. Today (1991) 173–301.
[7] D.G. Cantrell, L.J. Gillie, A.F. Lee, K. Wilson, Appl. Catal. A: Gen. 2 (2005) 183–190.
[8] W. Xie, H. Peng, L. Chen, J. Mol. Catal. A: Chem. 1–2 (2006) 24–32.
[9] J.L. Shumaker, C. Crofcheck, S.A. Tackett, E. Santillan-Jimenez, T. Morgan, Y. Ji, M. Crocker, T.J. Toops, Appl. Catal. B: Environ. 1–2 (2008) 120–130.
[10] U. Rashid, F. Anwar, Fuel 3 (2008) 265–273.
[11] S. Gryglewicz, Bioresour. Technol. (1999) 249–253.
[12] C.S. MacLeod, A.P. Harvey, A.F. Lee, K. Wilson, Chem. Eng. J. 1–2 (2008) 63–70.
[13] D.E. López, J.G. Goodwin Jr., D.A. Bruce, S. Furuta, Appl. Catal. A: Gen. 1 (2008) 76–83.
[14] J.M. Encinar, J.F. Gonzalez, J.J. Rodriguez, A. Tejedor, Energy Fuels (2002) 443–450.
[15] J. Pérez-Ramírez, G. Mul, F. Kapteijn, J.A. Moulijn, Mater. Res. Bull. 10 (2001) 1767–1775.
[16] M. Bellotto, B. Rebours, O. Clause, J. Lynch, D. Bazin, E. Elkaim, J. Phys. Chem. 20 (1996) 8535–8542.
[17] T. Hibino, A. Tsunashima, Clays and Clay Miner. 6 (1997) 842–853.
[18] R. Bîrjega, O.D. Pavel, G. Costentin, M. Che, E. Angelescu, Appl. Catal. A: Gen. 1–2 (2005) 185–193.
[19] S. Kannan, C.S. Swamy, Catal. Today 4 (1999) 725–737.

[20] L. Obalová, K. Pacultová, J. Balabánová, K. Jirátová, Z. Bastl, M. Valášková, Z. Lacný, F. Kovanda, Catal. Today 1–4 (2007) 233–238.
[21] D6584-00E0, Test Method for Determination of Free and Total Glycerin in B-100 Biodiesel Methyl Esters By Gas Chromatography in Annual Book of ASTM Standards, ASTM International, West Conshohocken, 2006.
[22] M. Bellotto, B. Rebours, O. Clause, J. Lynch, D. Bazin, E. Elkaim, J. Phys. Chem. 20 (1996) 8527–8534.
[23] J. Wittlinger, S. Werner, H. Schulz, Acta Crystallogr. Sect. B: Struct. Sci. 6 (1998) 714–721.
[24] P. Kustrowski, L. Chmielarz, E. Bozek, M. Sawalha, F. Roessner, Mater. Res. Bull. 2 (2004) 263–281.
[25] E. Li, V. Rudolph, Energy Fuels 1 (2008) 145–149.
[26] D. Kusdiana, S. Saka, Fuel 5 (2001) 693–698.
[27] H. Noureddini, D. Zhu, J. Am. Oil Chem. Soc. 11 (1997) 1457–1463.